

Longitudinal conductivity in ABC-stacked trilayer graphene under irradiating of linearly polarized light

Guo-Bao Zhu(朱国宝), Hui-Min Yang(杨慧敏), and Jie Yang(杨杰)

Citation: Chin. Phys. B, 2022, 31 (**8**): 088102. DOI: 10.1088/1674-1056/ac7205
Journal homepage: http://cpb.iphy.ac.cn; http://iopscience.iop.org/cpb

What follows is a list of articles you may be interested in

Photon-interactions with perovskite oxides

Hongbao Yao(姚洪宝), Er-Jia Guo(郭尔佳), Chen Ge(葛琛), Can Wang(王灿), Guozhen Yang(杨国桢), and Kuijuan Jin(金奎娟)
Chin. Phys. B, 2022, 31 (**8**): 088106. DOI: 10.1088/1674-1056/ac754c

Multiple bottle beams based on metasurface optical field modulation and their capture of multiple atoms

Xichun Zhang(张希纯), Wensheng Fu(付文升), Jinguang Lv(吕金光), Chong Zhang(张崇),Xin Zhao(赵鑫), Weiyan Li(李卫岩), and He Zhang(张贺)
Chin. Phys. B, 2022, 31 (**8**): 088103. DOI: 10.1088/1674-1056/ac4e06

Effects of electrical stress on the characteristics and defect behaviors in GaN-based near-ultraviolet light emitting diodes

Ying-Zhe Wang(王颖哲), Mao-Sen Wang(王茂森), Ning Hua(化宁), Kai Chen(陈凯), Zhi-Min He(何志敏), Xue-Feng Zheng(郑雪峰), Pei-Xian Li(李培咸), Xiao-Hua Ma(马晓华), Li-Xin Guo(郭立新), and Yue Hao(郝跃)
Chin. Phys. B, 2022, 31 (**6**): 068101. DOI: 10.1088/1674-1056/ac4cb8

Thermoelectric characteristics of flexible reduced graphene oxide/silver selenide nanowire composites prepared by a facile vacuum filtration process

Zuo Xiao(肖佐), Yong Du(杜永), Qiufeng Meng(孟秋风), and Lei Wang(王磊)
Chin. Phys. B, 2022, 31 (**2**): 028103. DOI: 10.1088/1674-1056/ac447e

Direct growth of graphene films without catalyst on flexible glass substrates by PECVD

Rui-Xia Miao(苗瑞霞), Chen-He Zhao(赵晨鹤), Shao-Qing Wang(王少青), Wei Ren(任卫), Yong-Feng Li(李永锋), Ti-Kang Shu(束体康), and Ben Yang(杨奔)
Chin. Phys. B, 2021, 30 (**9**): 098101. DOI: 10.1088/1674-1056/abeeec

---

Longitudinal conductivity in ABC-stacked trilayer graphene under irradiating of linearly polarized light

Guo-Bao Zhu(朱国宝)[1], Hui-Min Yang(杨慧敏)[1,†], and Jie Yang(杨杰)[2]

[1] *School of Physics and Electronic Engineering, Heze University, Heze* 274015, *China*
[2] *Shandong Graphenjoy Advanced Material Co. LTD, Dezhou* 253072, *China*

(Received 23 February 2022; revised manuscript received 18 May 2022; accepted manuscript online 23 May 2022)

We study the effect of linearly polarized light on the band structure and longitudinal conductivity in ABC-stacked trilayer graphene. The linearly polarized light can induce a pair of additional points in ABC-stacked trilayer graphene, where conduct and valence bands touch. The locations of these points are determined by the amplitude of the light. Furthermore, the layer pseudospin polarization can be controlled by the light. When the Fermi energy locates at Dirac points, i.e., $E_{\rm f} = 0$, the longitudinal conductivity shows resonance phenomena when the light is present. Away from the Dirac points, the longitudinal conductivity is unchanged as varying $E_{\rm f}$ for weak light field at larger Fermi energy, and the amplitude of longitudinal conductivity can be controlled by tuning the light field amplitude. Moreover, the effect of linearly polarized light on resonance phenomena in k-cubic Rashba–Dresselhaus system under the irradiating of linearly polarized light is discussed.

Keywords: graphene, light, Floquet

PACS: 81.05.Uf, 73.61.Wp, 73.43.Cd **DOI:** 10.1088/1674-1056/ac7205

1. Introduction

In recent years, trilayer graphene (TLG) has attracted a great deal of attention in condensed matter physics experimentally and theoretically due to the rise of graphene. In TLG, the stacking of three layers can be either ABA (Bernal-type)[1–4] and ABC (rhombohedral-type).[5–8] They have distinct electronic properties that are of interest both for fundamental science and for technological applications. The conduction and valence bands of ABC-stacked TLG have a approximately cubic dispersion and touch at the charge neutrality point.[6] Engineering of the band structure and understanding the corresponding transport properties of ABC-stacked TLG are critical to realize their applications. ABC-stacked TLG's chiral band structure results in three Landau level orbits with zero kinetic energy.[9] An electric field perpendicular to TLG has been shown to open a band gap in TLG.[10,11] In ABC-stacked TLG aligned with boron nitride, the electronic structure of flat bands can be induced by moiré sublattice and electric field.[12] The distinctive band structures can give rise to different transport properties. By using high-magnetic fields, Kumar *et al.*[13] have observed compelling evidence of the integer quantum Hall effect in TLG. In the presence of a perpendicular magnetic field, the ground state of ABC-stacked trilayer graphene is a uniform quantum Hall state where the electrons occupy the lowest unoccupied Landau level orbital index.[14] By tuning the interplay between the electric field and intrinsic spin coupling, a quantum spin Hall state or a quantum valley Hall state can occur in ABC-stacked TLG.[15] When ABC-stacked TLG is aligned with a hexagonal boron nitride substrate, quantum-Hall-like physics can be simulated by tuning a perpendicular electric field.[16] Chen *et al.*[17] have confirmed that the ABC-stacked TLG exhibits a large anomalous Hall signal at zero magnetic field in experiment. However, in previous research of transports properties in ABC-stacked TLG, the longitudinal conductivity has rarely been taken into account.

On the other hand, Floquet engineering[18–22] has emerged as a powerful method for the realization of novel quantum systems with exotic properties. A graphene lattice system subjected to circular driving has been studied theoretically in a variety of frameworks. A circularly polarized light can open a gap in the Dirac cone, which is predicted to lead to a dc Hall current[23] in graphene in the absence of a uniform magnetic field, and has been reported in experiment.[23] Lifshitz transitions,[24] a Floquet isolator,[25] and valley polarization[26] have been investigated in bilayer graphene using circularly polarized light. In twisted bilayer graphene, the circularly polarized light can be used to control the modulation of interlayer hopping.[27,28] An off-resonant circularly polarized light drives chirally stacked TLG into a Floquet Chern insulator.[8] Band flattening effects and band gap openings have been found in twisted TLG due to the presence of the circularly polarized light.[29] However, the linearly polarized light has rarely been taken into account in previous considerations of irradiating of light.

The study of longitudinal conductivity is one of most interesting field in transport in Dirac materials. It can lead to understanding of the mechanisms that contribute to the anoma-

†Corresponding author. E-mail: yangyhm@163.com
© 2022 Chinese Physical Society and IOP Publishing Ltd

lous Hall effect.[30,31] When graphene illuminated with circularly polarized light, longitudinal conductivity can be a realistic observable to detect light-induced Floquet band gaps.[32] Optical longitudinal conductivity can also be used to probe the topological phase transition.[33] Therefore, graphene is an important platform to find topological states for both scientific explorations and potential technological applications.

Given these background, we have studied the effects of linearly polarized light on ABC-stacked TLG. We have investigated the changes of band structure, layer pseudospin polarization, and longitudinal conductivity in ABC-stacked TLG when the light is present.

This paper is organized as follows. We firstly present the model Hamiltonian of TLG including the linearly polarized light, and analyze band structures in Section 2. Based on these results, we further obtain the evolution of layer pseudospin polarization in Section 3. The longitudinal conductivity is discussed in Section 4. In Section 5, we discuss the resonance phenomena in k-cubic Rashba–Dresselhaus system under the irradiating of linearly polarized light. Finally, we give a brief conclusion in Section 6.

2. Model Hamiltonian and energy spectrum

We begin the effective Hamiltonian of ABC-stacked TLG as follows:[5–8]

$$H = g_3 p^3[\cos(3\theta_p)\sigma_x + \sin(3\theta_p)\sigma_y], \tag{1}$$

where $g_3 = v_F^3/\gamma_1^2$, v_F is the Fermi velocity in graphene, γ_1 is the interlayer hopping energy; $\cos\theta_p = \eta p_x/p$, $\sin\theta_p = p_y/p$, $\eta = \pm 1$ labels valleys K and K'; $p_{x,y}$ are components of the momentum measured relative to the K/K' point. The Pauli matrices $\sigma_{x,y}$ act on the low-energy layer pseudospin degree of freedom, and $\sigma_\pm = \sigma_x \pm \mathrm{i}\sigma_y$.

When the system is subjected to an external time-dependent periodic perturbation in the form of light, the time-dependent vector potential is expressed as

$$\boldsymbol{A}(t) = A_0[\sin(\omega t), \sin(\omega t + \phi_0)], \tag{2}$$

where A_0 is the field amplitude, ω is the angular frequency of the irradiation, and ϕ_0 is the phase.

Previous works[18,34] proposed that light can dress the band structures of the system in high frequency regime, and the system can be described by static Hamiltonian. Based on the Floquet theory,[19–22] the static time independent Hamiltonian in high frequency limit is written as

$$H_{\mathrm{eff}} = H_0 + \frac{1}{\hbar\omega}[H_{-1}, H_1], \tag{3}$$

with

$$H_n = \frac{1}{T}\int_0^T \mathrm{d}t\, \mathrm{e}^{n\mathrm{i}\omega t} H(t), \tag{4}$$

where $T = 2\pi/\omega$ is the time period of the light. The Hamiltonian $H(t)$ is obtained by including the light induced vector potential into Hamiltonian (1) by $\boldsymbol{p} \to \boldsymbol{p} + e\boldsymbol{A}(t)/\hbar$, where $e < 0$ is the electron charge. For linearly polarized light ($\phi_0 = 0$), we obtain $H(t)$ in ABC-stacked TLG as

$$\begin{aligned} H(t) &= h_0 + h_x\sigma_x + h_y\sigma_x, && (5)\\ h_0 &= H - 3\eta g_3\kappa^2(p_y\sigma_x - p_x\sigma_y), && (6)\\ h_x &= \eta g_3\kappa[3(p_x^2 - p_y^2 - 2p_xp_y)\sin(\omega t) \\ &\quad - 2\kappa^2\sin^3(\omega t) + 2\kappa p_y\cos(2\omega t)], && (7)\\ h_y &= -g_3\kappa[3(p_y^2 - p_x^2 - 2p_xp_y)\sin(\omega t) \\ &\quad - 2\kappa^2\sin^3(\omega t) + 2\kappa p_x\cos(2\omega t)], && (8) \end{aligned}$$

where $\kappa = eA_0/\hbar$. For ABC-stacked TLG irradiated by linearly polarized light, the straightforward calculations show that $H_0 = h_0$ for $n = 0$, and the term $[H_{-1}, H_1]$ vanishes (see appendix A for details of calculations). Hence, the Hamiltonian irradiated by linearly polarized light can be simplified to

$$\begin{aligned} H_{\mathrm{eff}} &= g_3[(p^3\cos(3\theta_p) - 3\eta\kappa^2 p_y)\sigma_x \\ &\quad + (p^3\sin(3\theta_p) + 3\kappa^2 p_x)\sigma_y]. \end{aligned} \tag{9}$$

The corresponding eigenvalues and eigenvectors are

$$E_\pm = \pm g_3 p\sqrt{[p^2 + 3\kappa^2\cos(2\phi)]^2 + 9\kappa^4\sin^2(2\phi)}, \tag{10}$$

$$|u_{\pm\boldsymbol{p}}\rangle = [1, \pm\mathrm{i}\,\mathrm{e}^{-\mathrm{i}\chi}]^T/\sqrt{2}, \tag{11}$$

where $\tan\phi = p_y/p_x$, and $\tan\chi = \eta[3\kappa^2\sin\phi - p^2\cos(3\phi)]/[3\kappa^2\cos\phi + p^2\sin(3\phi)]$. It should be noted that the energy dispersions do not depend on the frequency of light, and they are valley degenerate and anisotropic for $\kappa \neq 0$. On the other hand, the conduction and valence bands touch at $(p, \phi) = (\sqrt{3}\kappa, \frac{\pi}{2})$ and $(p, \phi) = (\sqrt{3}\kappa, \frac{3\pi}{2})$ when the negative energy band is fully occupied and the positive one is empty. Figure 1 show the energy dispersions as functions of p in units of g_3 for (a) $\kappa = 0$ and (b) $\kappa = 0.2$ at $\phi = \pi/2$. It can be found that the linearly polarized light induces a pair of additional points away from $p = 0$, where conduct and valence bands touch.

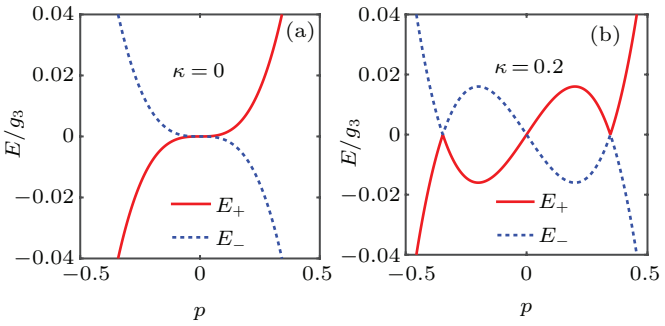


Fig. 1. Energy dispersions as functions of p in units of g_3 for (a) $\kappa = 0$ and (b) $\kappa = 0.2$ at $\phi = \pi/2$. The solid red and dotted blue curves are corresponding to E_+ and E_- respectively.

3. Layer pseudospin polarization

In this section, we investigate the effects of linearly polarized light on average layer pseudospin polarization. Based on Eq. (11), we can evaluate different components of the average layer pseudospin polarization as

$$\begin{aligned}\overline{s_{x\pm}} &= \pm\langle u_{\pm\boldsymbol{p}}|s_x|u_{\pm\boldsymbol{p}}\rangle = \pm\frac{p^2\cos(3\phi)-3\kappa^2\sin\phi}{\sqrt{p^4+6p^2\kappa^2\cos(2\phi)+9\kappa^4}}\\ &= g_3 p\frac{p^2\cos(3\phi)-3\kappa^2\sin\phi}{E_\pm}, \qquad (12)\\ \overline{s_{y\pm}} &= \pm\langle u_{\pm\boldsymbol{p}}|s_y|u_{\pm\boldsymbol{p}}\rangle = \pm\frac{p^2\sin(3\phi)+3\kappa^2\cos\phi}{\sqrt{p^4+6p^2\kappa^2\cos(2\phi)+9\kappa^4}}\\ &= g_3 p\frac{p^2\sin(3\phi)+3\kappa^2\cos\phi}{E_\pm}, \qquad (13)\end{aligned}$$

where $s_{x,y}=\hbar\sigma_{x,y}/2$, and $\pm$ denote conduct and valence bands, respectively. When the light field is absent, $\overline{s_{x\pm}}=\pm\cos(3\phi)$ and $\overline{s_{y\pm}}=\pm\sin(3\phi)$. At $E_{\rm f}=0$, Figs. 2(a) and 2(b) show that the average layer pseudospin polarization exhibits a peak at the location of additional points due to the present of the light field . In Fig. 3, we plot the layer pseudospin polarization $\overline{s_{x+}}$ [(a), (c)] and $\overline{s_{y+}}$ [(b), (d)] as functions of ϕ for $p=0.2$ [(a), (b)] and $p=0.6$ [(c), (d)] at different κ for $\eta=1$, respectively. When the irradiation of light is included, the average layer pseudospin polarization is significantly changed. Therefore, the irradiating of a light field on TLG can affect the transport properties of the system. Our results can provide a way to modify the transport properties of Dirac materials, and we will discuss the effects of linearly polarized light on the longitudinal conductivity in the next section.

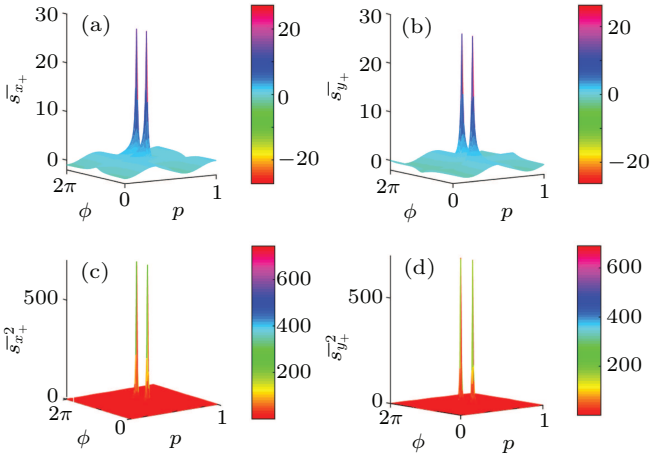


Fig. 2. $\overline{s_{x+}}$ (a), $\overline{s_{y+}}$ (b), $\overline{s_{x+}^2}$ (c), and $\overline{s_{y+}^2}$ (d) in the $(p,\phi/\pi)$ plane at $\kappa=0.1$.

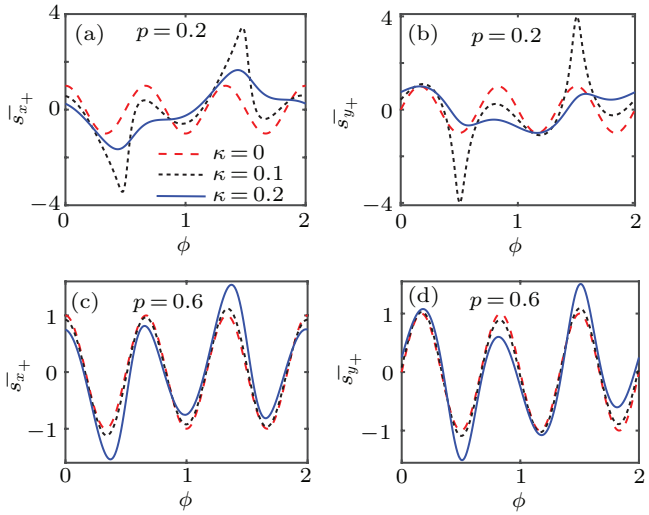


Fig. 3. Layer pseudospin polarization $\overline{s_{x+}}$ [(a), (c)] and $\overline{s_{y+}}$ [(b), (d)] as function of ϕ at different κ for $p=0.2$ [(a), (b)] and $p=0.6$ [(c), (d)], respectively. The red dashed, black dotted, and blue solid curves correspond to $\kappa=0$, $\kappa=0.1$, and $\kappa=0.2$ for $\eta=1$, respectively.

4. Longitudinal conductivity

In this section, we investigate the longitudinal conductivity of ABC-stacked TLG under the irradiating of linearly polarized light. Based on Green's function theory,[35–38] the longitudinal conductivity σ_{ii} can be expressed as

$$\begin{aligned}\sigma_{ii} = &-\frac{e\hbar}{2}\int\frac{{\rm d}\varepsilon}{2\pi}\partial_\varepsilon f(\varepsilon)\\ &\times\int\frac{{\rm d}^2\boldsymbol{p}}{(2\pi\hbar)^2}{\rm Tr}\big[v_i(\boldsymbol{p})G_0^{\rm R}(\varepsilon,\boldsymbol{p})v_i(\boldsymbol{p})(G_0^{\rm A}(\varepsilon,\boldsymbol{p})\\ &-G_0^{\rm R}(\varepsilon,\boldsymbol{p}))-v_i(\boldsymbol{p})(G_0^{\rm A}(\varepsilon,\boldsymbol{p})\\ &-G_0^{\rm R}(\varepsilon,\boldsymbol{p}))v_i(\boldsymbol{p})G_0^{\rm A}(\varepsilon,\boldsymbol{p})\big], \qquad (14)\end{aligned}$$

where $f(\varepsilon)$ is the Fermi distribution;

$$v_{x,y}=(1/\hbar)(\partial H_{\rm eff}/\partial p_{x,y})$$

is the velocity operator, and

$$G_0^{\rm R,A}(\varepsilon,\boldsymbol{p})=[\varepsilon-H_{\rm eff}(\boldsymbol{p})\pm{\rm i}0^+]^{-1} \qquad (15)$$

is the retarded (advanced) Green's function in the clean limit. In this paper, we consider the intrinsic contribution when the relaxation rate vanishes. Plugging Eq. (15) into Eq. (14), we can obtain

$$\begin{aligned}\sigma_{ii} = &-\frac{e^2\hbar}{2}\int\frac{{\rm d}\varepsilon}{2\pi}\partial_\varepsilon f(\varepsilon)\int\frac{{\rm d}^2\boldsymbol{p}}{(2\pi\hbar)^2}\sum_n\langle u_{n\boldsymbol{p}}|\hat{v}_x(\boldsymbol{p})|u_{m\boldsymbol{p}}\rangle\langle u_{m\boldsymbol{p}}|\hat{v}_x(\boldsymbol{p})|u_{n\boldsymbol{p}}\rangle\\ &\times\left[\frac{1}{\varepsilon-\varepsilon_m+{\rm i}0^+}-\frac{1}{\varepsilon-\varepsilon_m-{\rm i}0^+}\right]\left[\frac{1}{\varepsilon-\varepsilon_n-{\rm i}0^+}-\frac{1}{\varepsilon-\varepsilon_n+{\rm i}0^+}\right], \qquad (16)\end{aligned}$$

where ε_n is the eigenfunction of the effective Hamiltonian $H_{\rm eff}(\boldsymbol{p})$, and $|u_n\rangle$ is the corresponding eigenvalue. Base on the relation,

$\frac{1}{\varepsilon-\varepsilon_m\pm i0^+} = P\frac{1}{\varepsilon-\varepsilon_m} \mp i\pi\delta(\varepsilon-\varepsilon_m)$, the longitudinal conductivity can be written as

$$\sigma_{ii} = -\pi\hbar e^2 \int d\varepsilon \partial_\varepsilon f(\varepsilon) \int \frac{d^2\boldsymbol{p}}{(2\pi\hbar)^2} \sum_n \langle u_{n\boldsymbol{p}}|\hat{v}_x(\boldsymbol{p})|u_{m\boldsymbol{p}}\rangle\langle u_{m\boldsymbol{p}}|\hat{v}_x(\boldsymbol{p})|u_{n\boldsymbol{p}}\rangle \delta(\varepsilon-\varepsilon_n)\delta(\varepsilon-\varepsilon_m). \quad (17)$$

In the low-temperature regime, using the relation[39] $-df_0(\varepsilon)/d\varepsilon \approx \delta(E_F-\varepsilon)$, we obtain

$$\sigma_{ii} = \pi\hbar e^2 \int \frac{d^2\boldsymbol{p}}{(2\pi\hbar)^2} \sum_n \langle u_{n\boldsymbol{p}}|\hat{v}_x(\boldsymbol{p})|u_{n\boldsymbol{p}}\rangle^2 \delta(E_F-\varepsilon_n). \quad (18)$$

At $E_f = 0$, i.e., the negative energy band is fully occupied and the positive one is empty at zero temperature, we obtain $\sigma_{xx} = \frac{3}{4}\frac{e^2}{\hbar}$ when the linearly polarized light is absent. When the light field is included, σ_{xx} is determined by square of layer pseudospin polarization (see Eq. (18)). Figures 2(c) and 2(d) show that the resonance peaks occur in curves square of layer pseudospin polarization. Therefore, σ_{xx} shows a resonance phenomena. In Fig. 4, we plot the σ_{xx} as a function of Fermi energy E_f in units of $\sigma_0 = e^2/\hbar$ under the irradiating of linearly polarized light. When E_f sweeps away from the Dirac points, the σ_{xx} increases with E_f. We have considered a weak light field based on Floquet theory, and the κ is small. Therefore, σ_{xx} is unchanged for varying E_f at larger Fermi energy. Moreover, the amplitude of σ_{xx} can be controlled by κ.

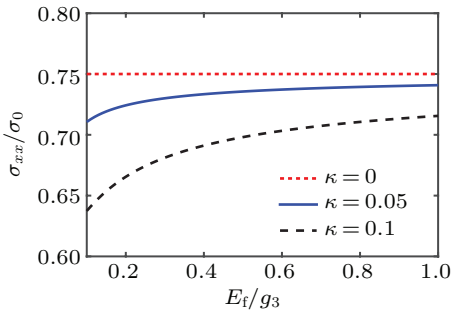


Fig. 4. Characteristics of σ_{xx} (in units of $\sigma_0 = e^2/\hbar$) as a function of E_f. The red dotted, blue solid, and black dashed curves correspond to $\kappa = 0$, $\kappa = 0.1$, and $\kappa = 0.2$, respectively.

5. Resonance phenomena in the *k*-cubic Rashba–Dresselhaus system under irradiating of linearly polarized light

Electronic structures of ABC-stacked trilayer graphene exhibit a k-cubic dispersion relation, and show resonance phenomena when the linearly polarized light is present. Another interesting way to include the k-cubic term is considering spin orbit coupling. In this section, we consider the k-cubic Rashba–Dresselhaus system under the irradiating of linearly polarized light. For the k-cubic Rashba–Dresselhaus system, the Hamiltonian[40,41] is given by

$$\hat{H}_0^{SO} = \frac{\hbar^2k^2}{2m} + \frac{i\alpha}{2}(k_-^3\tau_+ - k_+^3\tau_-) - \frac{\beta}{2}(k_-^2k_+\tau_+ + k_+^2k_-\tau_-), \quad (19)$$

where m is effective mass, and $k_\pm = k_x \pm ik_y$ with $k_{x,y}$ being momentums along the x and y axes respectively; $\tau_\pm = \tau_x \pm i\tau_y$ with Pauli matrices $\tau_{x,y}$ acting on spin degree of freedom; α and β denote the cubic Rashba and Dresselhaus spin orbit strengths, respectively. Based on Eq. (4), the effective Hamiltonian under the irradiating of linearly polarized light is (see appendix B for details of calculations)

$$\hat{H}_{eff}^{SO} = \hat{H}_0^{SO} - \alpha\kappa^2(k_x\tau_x + k_y\tau_y) - \beta\kappa^2[(2k_x+k_y)\tau_x + (k_x+2k_y)\tau_y]. \quad (20)$$

The mentioned effective Hamiltonian can always be expressed in terms of the Pauli matrices as

$$\hat{H}_0^{SO} = d_0\boldsymbol{I} + d_x\tau_x + d_y\tau_y, \quad (21)$$

where $d_0 = \frac{\hbar^2k^2}{2m}$, and $\boldsymbol{I}$ is the rank-2 unit matrix; $d_x = \alpha(3k_x^2k_y - k_y^3 - \kappa^2k_x) - \beta(k^2k_x + 2\kappa^2k_x + \kappa^2k_y)$, and $d_x = \alpha(k_x^3 - 3k_xk_y^2 - \kappa^2k_y) - \beta(k^2k_y + \kappa^2k_x + 2\kappa^2k_y)$. The corresponding eigenvalues and eigenvectors are

$$E_n^{SO} = d_0 + (-1)^n\sqrt{d_x^2+d_y^2}, \quad (22)$$

$$|n\rangle = e^{(-1)^n i\frac{\gamma}{2}}\left[\sin\left(\frac{\gamma}{2}+\pi\frac{n-1}{2}\right)e^{i\frac{\gamma}{2}} - \cos\left(\frac{\gamma}{2}+\pi\frac{n-1}{2}\right)e^{-i\frac{\gamma}{2}}\right]^T, \quad (23)$$

where $n = 1,2$ denote the spin down (up) band, superscript T denotes the transpose of the matrix, and $\tan\gamma = d_y/d_x$. Moreover, the average spin polarization can be obtained as $\overline{s_{x,n}^{so}} = nd_x/(E_n^{SO} - d_0)$ and $\overline{s_{y,n}^{so}} = nd_y/(E_n^{SO} - d_0)$. Furthermore, based on Eq. (18), the longitudinal conductivity is related to $a\overline{s_{x,n}^{so}}^2 + b\overline{s_x^{so}}\,\overline{s_{y,n}^{so}} + b\overline{s_{y,n}^{so}}^2$ with $\boldsymbol{k}$-depended parameters a,b,c.

When the cubic Dresselhaus spin orbit is absent ($\beta = 0$), the system is similar with ABC-stacked trilayer graphene except the kinetic energy term $k^2/2m$. However, the kinetic energy term does not change the eigenvectors of the system. Therefore, the average spin polarization of the case is same as that in ABC-stacked trilayer graphene, and a pair of additional points occurs in the system [see Fig. 5(a)].

When the cubic Rashba spin orbit is absent ($\alpha = 0$), based on Eq. (22), the energy difference $\Delta = E_2^{SO} - E_1^{SO}$ is zero only when $\boldsymbol{k} = 0$ [see Fig. 5(a)]. Therefore, there is no additional point for the system, and the resonance phenomena will be absent. These are different from that in ABC-stacked trilayer graphene.

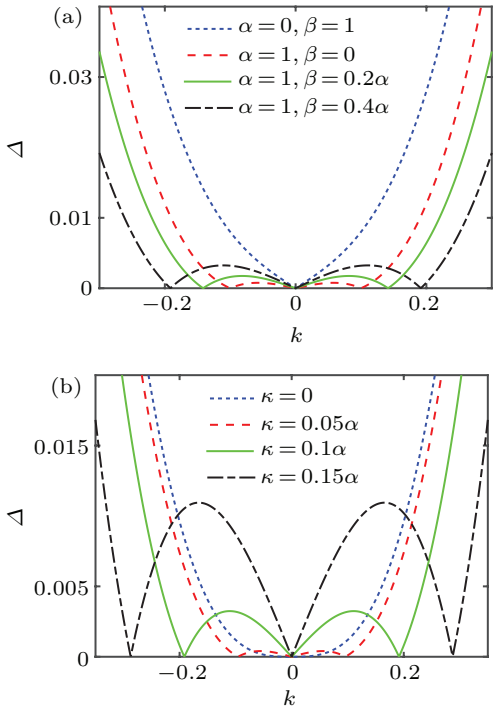


Fig. 5. (a) $\Delta = E_2^{\rm SO} - E_1^{\rm SO}$ as functions of k at $\gamma = \pi/4$ with different α and β. (b) Δ as functions of k at $\gamma = \pi/4$ and $\beta = 0.4\alpha$ with different κ.

When both the cubic Rashba and Dresselhaus spin orbit are included ($\alpha \neq 0, \beta \neq 0$), Fig. 5(a) shows $\Delta = E_2^{\rm SO} - E_1^{\rm SO}$ as functions of k at $\gamma = \pi/4$ with different α and β. The locations of additional points can be controlled by tuning the strength of spin orbit coupling. Δ as functions of k at $\gamma = \pi/4$ and $\beta = 0.4\alpha$ with different κ are plotted in Fig. 5(b). Tuning the amplitude of the linearly polarized light can change the locations of additional points in the system. Therefore, the k-cubic Rashba–Dresselhaus system also exhibits resonance phenomena, which occur in ABC-stacked trilayer graphene. However, in the k-cubic Rashba–Dresselhaus system, the resonance phenomena can be controlled by the interplay between cubic Rashba, Dresselhaus spin orbits and linearly polarized light.

6. Conclusions

We have shown that the linearly polarized light can induce the change of the band structure and longitudinal conductivity in ABC-stacked trilayer graphene. Most remarkably, the band structure of ABC-stacked trilayer graphene exhibits a pair of additional points, where conduct and valence bands touch. The points are responsible for the resonance phenomena of the longitudinal conductivity. The amplitude of linearly polarized light can be used to tune the locations of the additional points. Furthermore, the layer pseudospin polarization is sensitive to the light. At the larger Fermi energy, the longitudinal conductivity is unchanged for varying $E_{\rm f}$, and the amplitude of σ_{xx} can be controlled by changing κ. We present the results of resonance phenomena in the k-cubic Rashba–Dresselhaus system under irradiating of linearly polarized light. Our results provide a way to control transport properties of Dirac materials.

Appendix A: Floquet Hamiltonian

Based on Eq. (4), when the linearly polarized light is included, we can obtain

$$H_{\pm 1} = \frac{1}{T}\int_0^T {\rm d}t\, {\rm e}^{\pm {\rm i}\omega t}[H_1^x\sigma_x + H_1^y\sigma_x], \tag{A1}$$

$$H_1^x = \frac{3\eta g_3}{4}\kappa[2{\rm i}(p_x^2 - p_y^2 - 2p_xp_y)\sin(\omega t) - {\rm i}\kappa^2\sin^3(\omega t) + 2\kappa p_y\cos(2\omega t)], \tag{A2}$$

$$H_1^y = -\frac{3g_3}{4}\kappa[2{\rm i}(p_y^2 - p_x^2 - 2p_xp_y)\sin(\omega t) - {\rm i}\kappa^2\sin^3(\omega t) + 2\kappa p_x\cos(2\omega t)], \tag{A3}$$

$$H_1 = -H_{-1}, \tag{A4}$$

where we have used the relations

$$\frac{1}{T}\int_0^T {\rm d}t\, {\rm e}^{\pm {\rm i}\omega t}\sin(\omega t) = \pm\frac{\rm i}{2}, \tag{A5}$$

$$\frac{1}{T}\int_0^T {\rm d}t\, {\rm e}^{\pm {\rm i}\omega t}\sin^3(\omega t) = \pm\frac{3{\rm i}}{8}, \tag{A6}$$

$$\frac{1}{T}\int_0^T {\rm d}t\, {\rm e}^{\pm {\rm i}\omega t}\cos(2\omega t) = 0. \tag{A7}$$

Then, we obtain

$$[\hat{H}_1, \hat{H}_{-1}] = 0. \tag{A8}$$

Appendix B: Floquet Hamiltonian of the k-cubic Rashba–Dresselhaus system

When the linearly polarized light $\boldsymbol{A}(t) = A_0[\sin(\omega t), \sin(\omega t)]$ is included, the cubic Rashba–Dresselhaus spin orbit coupled Hamiltonian is

$$\hat{H}_0^{\rm SO}(t) = \hat{H}_0^{\rm RSO} - \alpha\kappa^2(k_x\tau_x + k_y\tau_y) - \beta\kappa^2[(2k_x + k_y)\tau_x + (k_x + 2k_y)\tau_y] + (H_x^{\rm RSO} + H_x^{\rm DSO})\tau_x + (H_y^{\rm RSO} + H_y^{\rm DSO})\tau_y, \tag{B1}$$

where

$$H_x^{\rm RSO} = \alpha[3(k_y^2 - k_x^2 - 2k_xk_y)\kappa\sin(\omega t) - 2\kappa^3\sin^3(\omega t) + 3\kappa^2k_x\cos(2\omega t)], \tag{B2}$$

$$H_y^{\rm RSO} = \alpha[3(k_x^2 - k_y^2 - 2k_xk_y)\kappa\sin(\omega t) - 2\kappa^3\sin^3(\omega t) + 3\kappa^2k_y\cos(2\omega t)], \tag{B3}$$

$$H_x^{\rm DSO} = \beta[(3k_x^2 + k_y^2 + 2k_xk_y)\kappa\sin(\omega t) + 2\kappa^3\sin^3(\omega t) - (2k_x + k_y)\kappa^2k_x\cos(2\omega t)], \tag{B4}$$

$$H_y^{\rm DSO} = \beta[(3k_y^2 + k_x^2 + 2k_xk_y)\kappa\sin(\omega t) + 2\kappa^3\sin^3(\omega t) - (k_x + 2k_y)\kappa^2k_x\cos(2\omega t)]. \tag{B5}$$

Based on Eqs. (4) and (A5)–(A7), we obtain

$$[\hat{H}_1^{\rm SO}, \hat{H}_{-1}^{\rm SO}] = 0. \tag{B6}$$

Then the Floquet hamiltonian of topological insulator with hexagonal warping is

$$\hat{H}_{\rm eff}^{\rm SO} = \hat{H}_0^{\rm SO} - \alpha\kappa^2(k_x\tau_x + k_y\tau_y) - \beta\kappa^2[(2k_x + k_y)\tau_x + (k_x + 2k_y)\tau_y]. \quad \text{(B7)}$$

Acknowledgement

Project supported by the Shandong Provincial Natural Science Foundation (Grant No. ZR2021MA093).

References

[1] Koshino M and McCann E 2013 *Phys. Rev. B* **87** 045420
[2] Guinea F, Castro Neto A H and Peres N M R 2006 *Phys. Rev. B* **73** 245426
[3] Koshino M and McCann E 2009 *Phys. Rev. B* **79** 125443
[4] Gelderen R, Lim L and Smith C M 2011 *Phys. Rev. B* **84** 155446
[5] Min H and MacDonald A H 2008 *Phys. Rev. B* **77** 155416
[6] Zhang F, Sahu B, Min H and MacDonald A H 2010 *Phys. Rev. B* **82** 035409
[7] Zhang F, Jung J, Fiete G A, Niu Q and MacDonald A H 2011 *Phys. Rev. Lett.* **106** 156801
[8] Li S, Liu C C and Yao Y 2018 *New J. Phys.* **20** 033025
[9] Barlas Y, Côté R and Rondeau M 2012 *Phys. Rev. Lett.* **109** 126804
[10] Lui C H, Li Z, Mak K F, Cappelluti E and Heinz T F 2011 *Nat. Phys.* **7** 944
[11] Zou K, Zhang F, Clapp C, MacDonald A H and Zhu J 2013 *Nano Lett.* **13** 369
[12] Chittari B L, Chen G, Zhang Y, Wang F and Jung J 2019 *Phys. Rev. Lett.* **122** 016401
[13] Kumar A, Escoffier W, Poumirol J M, Faugeras C, Arovas D P, Fogler M M, Guinea F, Roche S, Goiran M and Raquet B 2011 *Phys. Rev. Lett.* **107** 126806
[14] Côtè R, Rondeau M, Gagnon A M and Barlas Y 2012 *Phys. Rev. B* **86** 125422
[15] Rehman M U and Abid A A 2017 *Chin. Phys. B* **26** 127304
[16] Zhang Y H and Senthil T 2019 *Phys. Rev. B* **99** 205150
[17] Chen G, Sharpe A L, Fox E J, Zhang Y H, Wang S, Jiang L, Lyu B, Li H, Watanabe K, Taniguchi T, Shi Z, Senthil T, Gordon D G, Zhang Y and Wang F 2020 *Nature* **579** 56
[18] Oka T and Aoki H 2009 *Phys. Rev. B* **79** 081406
[19] Shirley J H 1965 *Phys. Rev.* **138** 979
[20] Sambe H 1973 *Phys. Rev. A* **7** 2203
[21] Grifoni M and Hänggi P 1998 *Phys. Rep.* **304** 229
[22] Kohler S, Lehmann J and Hänggi P 2005 *Phys. Rep.* **406** 379
[23] McIver J W, Schulte B, Stein F U, Matsuyama T, Jotzu G, Meier G and Cavalleri A 2020 *Nat. Phys.* **16** 38
[24] Iorsh I V, Dini K, Kibis O V and Shelykh I A 2017 *Phys. Rev. B* **96** 155432
[25] Lago V D, E. Morell S and Torres L E F F 2017 *Phys. Rev. B* **96** 235409
[26] Friedlan A and Dignam M M 2021 *Phys. Rev. B* **103** 075414
[27] Vogl M, Rodriguez-Vega M and Fiete G A 2020 *Phys. Rev. B* **101** 235411
[28] Vogl M, Rodriguez-Vega M and Fiete G A 2020 *Phys. Rev. B* **101** 241408
[29] Assi I A, LeBlanc J P F, Rodriguez-Vega M, Bahlouli H and Vogl M 2021 *Phys. Rev. B* **104** 195429
[30] Endo A, Hatano N, Nakamura H and Shirasaki R 2009 *J. Phys.: Condens. Matter* **21** 345803
[31] Mak K F, McGill K L, Park J and McEuen P L 2014 *Science* **344** 1489
[32] Broers L and Mathey L 2021 *Commun. Phys.* **4** 248
[33] Tan C Y, Yan C X, Zhao Y H, Guo H and Chang H R 2021 *Phys. Rev. B* **103** 125425
[34] Lindner N H, Rafael G and Galitski V 2011 *Nat. Phys.* **7** 490
[35] Onoda S, Sugimoto N and Nagaosa N 2006 *Phys. Rev. Lett.* **97** 126602
[36] Onoda S, Sugimoto N and Nagaosa N 2008 *Phys. Rev. B* **77** 165103
[37] Kovalev A A, Tserkovnyak Y, Vyborny K and Sinova J 2009 *Phys. Rev. B* **79** 195129
[38] Kovalev A A, Sinova J and Tserkovnyak Y 2010 *Phys. Rev. Lett.* **105** 036601
[39] Smrčka L and Středa P 1977 *J. Phys. C: Solid State Phys.* **10** 2153
[40] Alidoust M, Shen C and Žutić Igor 2021 *Phys. Rev. B* **103** L060503
[41] Chen T W and Hsu H C 2021 *New J. Phys.* **23** 073017